Spectroscopic Evidence for the Localization of Skyrmions near $\nu = 1$ as $T \rightarrow 0$

P. Khandelwal,[1] A. E. Dementyev,[1] N. N. Kuzma,[1] S. E. Barrett,[1] L. N. Pfeiffer,[2] and K. W. West[2]

[1]*Department of Physics, Yale University, New Haven, Connecticut 06511*
[2]*Bell Laboratories, Lucent Technologies, Murray Hill, New Jersey 07974*
(Received 11 September 2000)

Optically pumped nuclear magnetic resonance measurements of ^{71}Ga spectra were carried out in an n-doped GaAs/Al$_{0.1}$Ga$_{0.9}$As multiple quantum well sample near the integer quantum Hall ground state $\nu = 1$. As the temperature is lowered (down to $T \approx 0.3$ K), a "tilted plateau" emerges in the Knight shift data, which is a novel experimental signature of quasiparticle localization. The dependence of the spectra on both T and ν suggests that the localization is a collective process. The frozen limit spectra appear to rule out a 2D lattice of conventional Skyrmions.

One of the most surprising twists in the recent history of the quantum Hall effects [1] was the prediction [2] that novel spin textures called Skyrmions can be the charged quasiparticles introduced by small deviations ($|\delta\nu|$) from ferromagnetic quantum Hall ground states [3] (e.g., at Landau level filling factor $\nu = 1$ or $\frac{1}{3}$). A Skyrmion has an effective number of spin reversals K and "size" λ that are determined by the competition between the Coulomb energy (which increases both) and the Zeeman energy (which reduces both). Qualitatively, this cylindrically symmetric spin texture has a down spin at $r = 0$ and a smooth radial transition to up spins at $r = \infty$. In between, the nonzero XY spin components have a vortical configuration [2,4]. The addition of Skyrmions to the $\nu = 1$ ground state was predicted to result in a rapid drop in the electron spin polarization, as $|\delta\nu|$ is increased [5]. Several experiments are consistent with this [6–8] and other predictions [9–13] of the Skyrmion model.

These developments stimulated many theoretical studies of Skyrmions. One of the central questions that emerged was the nature of the many-Skyrmion ground state. Would Skyrmions form a crystal [14–20], and, if so, what symmetries would it possess? Does disorder [21] affect the Skyrmion size λ and spin number K as $T \rightarrow 0$? While these questions are still under active investigation, basic aspects of the Skyrmion model have not yet been tested experimentally. For example, the detailed shape of a Skyrmion has not yet been measured with local probes, presumably because the quasiparticles are delocalized at high T.

In this Letter, we report the first spectroscopic evidence for Skyrmion localization. The multiple quantum well sample used in this work was previously studied at higher temperatures [6,10]. The new data presented here were obtained by extending the optically pumped nuclear magnetic resonance (OPNMR) technique [22] to lower temperatures ($T \approx 0.3$ K) as described elsewhere [23,24].

Figure 1 shows some OPNMR spectra for ν close to one. Nuclei within the quantum wells are coupled to the spins of the two-dimensional electron system via the isotropic Fermi contact interaction [25], which shifts the corresponding well resonance (labeled "W" on Fig. 1c) relative

to the signal from the barriers ("B") [6,24]. We define the Knight shift K_S as the peak-to-peak splitting between W and B. The third resonance (labeled "X" in Fig. 1c) may be due to nuclei near "defect" sites. By scaling equilibrium signal intensities, we estimate that X is due to only $\sim2\%$ of quantum well nuclei [26]; for now we ignore it.

For $\nu = 1$, all spectra (e.g., Fig. 1c) are well described by the same two-parameter fit (dotted lines) [23,24] that was previously used for all spectra at $\nu = \frac{1}{3}$. Note that this fitting function has no explicit dependence on the (x, y) position of nuclei along the quantum well, despite the fact that NMR is a local probe. This is because the fit is generated under the assumption that all electron spins are *delocalized*, so that $\langle S_z(\nu, T)\rangle$, averaged over the NMR time scale (~20 μsec), appears spatially homogeneous along the plane of the wells, and thus the resulting line shape is
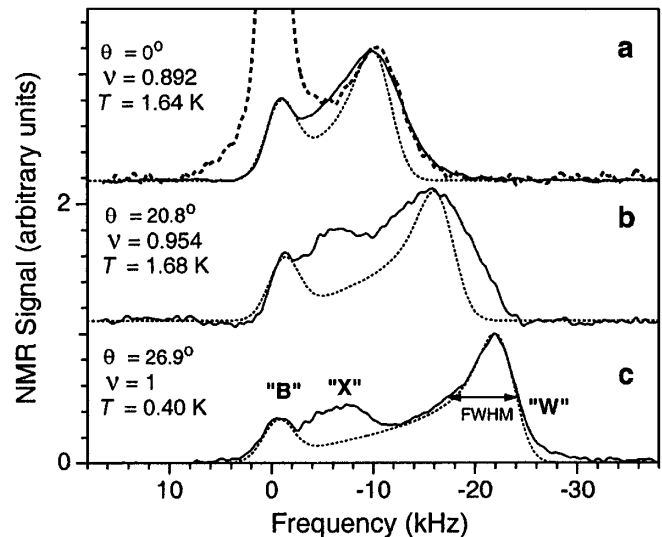

FIG. 1.   Several ^{71}Ga OPNMR emission spectra [(a)–(c), solid lines, offset for clarity], acquired at low T for different ν, in $B_{\text{tot}} = 7.03$ T ($f_o = 91.36$ MHz). The same "W" resonance is obtained using either conventional NMR absorption [(a), dashed line] or OPNMR emission [(a), solid line]. The dotted lines [(a)–(c)] are fits to W and "B," which assume identical quantum wells (see text).

"motionally narrowed" [25]. In this limit, measurement of K_S reveals the "global," time-averaged value of the electron spin polarization $\mathcal{P}$. On the other hand, for $\nu \neq 1$ and low T, the well resonance W (Figs. 1a and 1b) can also be much broader than this same fit (dotted lines).

Figure 2 shows the $K_S(\nu)$ and the $\Gamma_w(\nu)$ of the W resonance near $\nu = 1$, for three different temperatures. As the temperature is lowered (Figs. 2a–2c), the sharp peak in $K_S(\nu)$ evolves into a "tilted plateau." Figure 2b also contains the $K_S(\nu)$ data points reported previously [6]. While the new data are consistent with the earlier measurements, probing $K_S(\nu)$ on this finer scale reveals a small region on both sides of $\nu = 1$ where $K_S(\nu) \approx K_S(\nu = 1)/\nu$ (dashed line in Fig. 2c). This tilted plateau is incompatible with the expression for $K_S(\nu)$ derived previously [6], which had assumed *delocalized quasiparticles* [27]. The existence of the tilted plateau is a natural consequence of the localization of the quasiparticles along the plane of the quantum well, such that the nuclei responsible for the W resonance see fully polarized electrons ($\mathcal{P} = 1$), as if $\nu = 1$ "locally," even though $\nu \neq 1$ "globally." More precisely, for nuclei at $\mathbf{R_i} = (X', Y', Z' = 0)$ in the center of the quantum well, the local $K_{S\text{int}}(\mathbf{R_i})$ is directly proportional to the z component of the local electron spin magnetization density, $M_z(\mathbf{R_i})$ [25], which is in turn proportional to the product of the electron number density and the spin polarization, i.e., $M_z(\mathbf{R_i}) \propto |\phi(\mathbf{R_i})|^2 \mathcal{P}(\mathbf{R_i})$ [24]. If the quasiholes (or quasiparticles) introduced into the system by going to $\nu = 1 - \epsilon$ (or $\nu = 1 + \epsilon$) are localized, then, in order to keep the total number of electrons fixed, $|\phi(\mathbf{R_i})|^2$ *must* increase (or decrease) far from these charged excitations, which produces the observed

tilt in the plateau near $\nu = 1$. This is just the same effect as the rise (or fall) of the water level in a pool induced by placing solid dipsticks (or hollow capillary tubes) into it to create localized density minima (or maxima), which correspond to quasiholes (or quasiparticles). In this analogy, changing the filling factor by adjusting $B_{\text{tot}} \cos\theta$ varies the number of dipsticks or capillary tubes in the pool and the Knight shift is given by the water level. Clearly, the fact that NMR is a local probe has become important.

Taking different slices through the (ν, T) plane provides additional insights. Figure 3 shows $K_S(T)$ and $\Gamma_w(T)$ for several filling factors near $\nu = 1$. For $\nu \neq 1$, lowering the temperature causes $\Gamma_w(T)$ first to increase and then to drop, in stark contrast to the temperature independence of the well linewidth at $\nu = 1$. The nonmonotonic temperature dependence (Fig. 3) is consistent with the evolution of the W resonance from motionally narrowed to frozen as the temperature is lowered. Qualitatively similar trends were uncovered in earlier measurements at $\nu < 1/3$ [24]. Both cases are rather unusual examples of motional narrowing phenomena in NMR, since the nuclei are fixed in the lattice at such low T. Instead, the motion is that of delocalized spin-reversed quasiparticles that results in fluctuations of the local hyperfine field $\delta B_z^e(\mathbf{R_i})$ at each nuclear site $\mathbf{R_i}$. The shape of the resonance is sensitive to $\Theta(\mathbf{R_i}) \equiv \tau(\mathbf{R_i})\delta B_z^e(\mathbf{R_i})^i\gamma$, where $\tau(\mathbf{R_i})$ is the characteristic time scale of the fluctuations, and $^i\gamma$ is the nuclear gyromagnetic ratio [25]. As T is lowered, the W resonance goes from the motionally narrowed limit [at high T, $\Theta(\mathbf{R_i}) \ll 1$] to the "intermediate limit" [at T near $T_{\max}$, where $\Gamma_w(T_{\max}) = \Gamma_w^{\max}$, $\Theta(\mathbf{R_i}) \sim 1$] and then to the "frozen limit" [at low T, $\Theta(\mathbf{R_i}) \gg 1$]. Figures 2 and 3
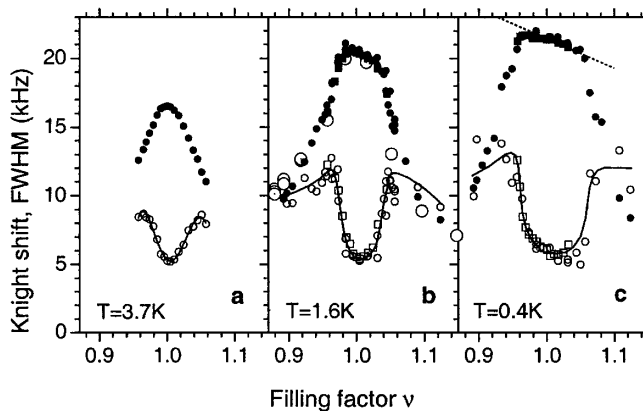

FIG. 2. $K_S(\nu)$ (solid symbols) and $\Gamma_w(\nu)$ (small open symbols) at (a) $T = 3.7$ K, (b) $T = 1.6$ K, and (c) $T = 0.4$ K. The large open symbols in (b) are K_S data previously reported for this sample. Here Γ_w is the full width at half maximum (FWHM) for the "W" resonance. The filling factor [$\nu = nhc/(eB_{\text{tot}} \cos\theta)$] is varied *in situ* by tilting the sample ($0° \leq \theta \leq 37°$). In practice, all the low temperature ($T < 1.6$ K) data were acquired following a cooldown from at least 1.6 K *at fixed* ν. The 2D electron density ($n = 1.52 \times 10^{11}$ cm^{-2}) is inferred from the $K_S(\nu)$ peak in (a). Solid lines are to guide the eye, and the dashed line is described in the text.
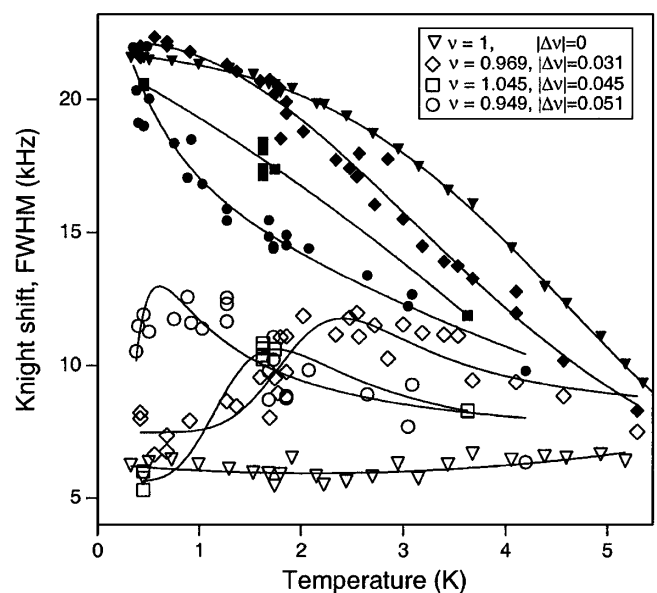

FIG. 3. $K_S(T)$ (filled symbols) and $\Gamma_w(T)$ (open symbols) for several filling factors $0.949 \leq \nu \leq 1.045$. Lines through $K_S(T)$ are to guide the eye. Lines through $\Gamma_w(T)$ are fits suggested by a simple model for Skyrmion dynamics (see text).

show that all three limits are experimentally accessible near $\nu = 1$.

Qualitatively, the $|\delta\nu|$ dependence of $\Gamma_w(T)$ (Fig. 3) appears to rule out several candidate mechanisms for the localization. For example, if *individual* Skyrmions were strongly pinned by a distribution of traps, then, as $\delta\nu$ increases, quasiparticles should "start" to localize at the same temperature, but "finish" at lower and lower temperatures. In contrast, as $\delta\nu$ increases, the whole $\Gamma_w(T)$ peak shifts to lower T (Fig. 3); e.g., at $T \approx 1.5$ K, all Skyrmions can appear to be either localized (at $|\delta\nu| = 0.031$) or delocalized (at $|\delta\nu| = 0.051$). We conclude that a *collective* process is required to explain the trends in Figs. 2 and 3. This process, however, does not appear to be the "melting" of a classical Skyrmion crystal, since the classical melting temperature should increase as the crystal density (and the bond energy) increases. Two other collective mechanisms are qualitatively consistent with the data. In the first scenario, the data are explained by the thermally assisted melting of a quantum Skyrmion crystal, which is approaching a quantum melting transition [28] at some $|\delta\nu| > 0.05$.

In the second, the delocalization is due to the "depinning" of a Skyrmion crystal, since the soft (stiff) bonds of the crystal at low (high) $|\delta\nu|$ may easily (not easily) stretch to match the disorder potential, resulting in a high (low) depinning temperature [29].

Additional, quantitative information about the localization process [26] may be obtained by simulating the effect of Skyrmion dynamics on the OPNMR spectra [26,30]. For example, to explain the $\Gamma_w(T, |\delta\nu| = 0.031)$ data, we require $K \approx 3$ even as $\Theta \to 1$ from below; the Skyrmion still has a "large" spin even as it takes $\sim 20~\mu s$ to travel over the inter-Skyrmion spacing. Furthermore, in simulations that assume spatially uniform local field fluctuations, we obtain Γ_w^{max} values that grow with increasing $|\delta\nu|$, as seen in earlier measurements [24]. In contrast, Fig. 3 shows that Γ_w^{max} is essentially constant for $0.031 < |\delta\nu| < 0.051$. Apparently, the actual localization process causes local field fluctuations that become more inhomogeneous as $|\delta\nu|$ increases [31].

In the frozen limit, the fit previously used for the motionally narrowed OPNMR spectrum [23,24] is replaced by the more general formula:

$$I(f) = a_b g(f) + \sum_{\mathbf{R_i}}^{area} \int_0^{K_{Sint}(\mathbf{R_i})} df' \, g(f - f') I_w^{int}(K_{Sint}(\mathbf{R_i}), f') \tag{1}$$

where the sum runs over all nuclei in the center of the quantum well, and $K_{Sint}(\mathbf{R_i}) \propto M_z(\mathbf{R_i})$, which in turn reflects the shape of individual quasiparticles and their spatial arrangement along the plane of the quantum well. Since conventional Skyrmions are expected to form a square lattice, we consider this possibility first.

Several theoretical approaches have been used to calculate $M_z(\mathbf{R_i})$ for a *single* Skyrmion excitation of the $\nu = 1$ ground state. Figure 4a shows the typical radial dependence of the dimensionless $M_z'(r)$ expected [4] for Skyrmions with $K = 0$ ("K0") and $K = 3$ ("K3") reversed spins. The K0 Skyrmion corresponds to the ordinary Laughlin quasiparticle, while both theory and experiment suggest that the K3 Skyrmion is energetically preferred for typical experimental conditions. Also shown in Fig. 4a is an *ad hoc* hybrid between the two ("K3*") that has both the tail of K0 and the three reversed spins of K3.

We approximate $M_z(\mathbf{R_i})$ for N localized Skyrmions with $M_z^{sim}(\mathbf{R_i})$ (Figs. 4b–4d). Using Eq. (1), we simulate the frozen limit OPNMR spectrum at $\nu = 1 + \delta\nu$, for various Skyrmion shapes. Figure 5 shows $[K_S^{sim}(\nu), \Gamma_w^{sim}(\nu)]$ extracted from these simulations, which may be quantitatively compared to the low temperature data of Fig. 2c. We can *rule out* the standard model of a square lattice of conventional K3 Skyrmions over most of the plateau (see Figs. 5a and 5b); using smaller conventional Skyrmions (K2, K1) helps, but not enough. Instead, the data are in much better agreement with simulations assuming a square lattice of either K0 or *ad hoc* K3* Skyrmions. Apparently, the existence of the tilted plateau requires that
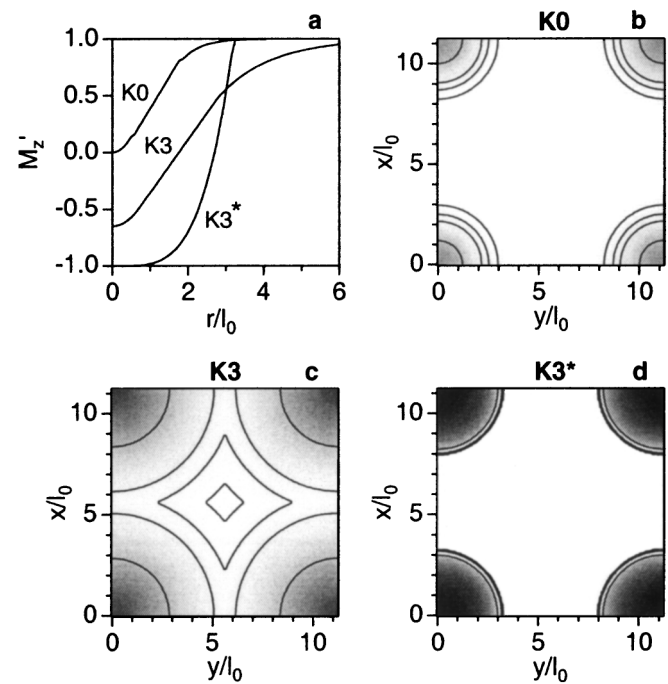

FIG. 4. (a) Expected radial dependence (in units of the magnetic length l_o) of $M_z'(r)$, for the K0, K3, and K3* Skyrmions described in the text. For $|\delta\nu| = 0.05$, gray scale images of $M_z^{sim}(\mathbf{R_i})$ (black $= -1$, white $= +1$) are shown within the unit cell of a square lattice of (b) K0, (c) K3, or (d) K3* Skyrmions. Also shown [in (b)–(d)] are black contour lines at $M_z^{sim} = 0.5$, 0.9, 0.95, and 0.98.
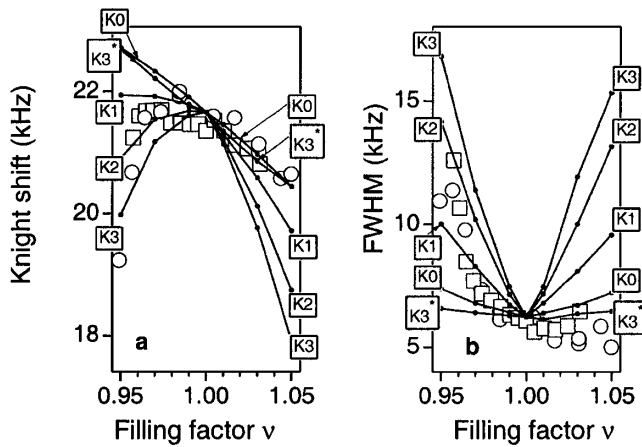
FIG. 5. Open symbols are $[K_S(\nu), \Gamma_w(\nu)]$ data from Fig. 2c. Filled points are $[K_S^{sim}(\nu), \Gamma_w^{sim}(\nu)]$ extracted from simulations described in the text. The points for each Skyrmion type are joined by lines.

$M_z^{sim}(\mathbf{R_i}) \sim 1$ over a large fraction of the area between the quasiparticles, as in Figs. 4b and 4d. This conclusion is not sensitive to the details of our simulation over the range ($|\delta\nu| \leq 0.05$) of the observed plateau (e.g., changing to a triangular lattice, or including small disorder in Skyrmion locations). If the localized state is a 2D lattice of quasiparticles, it appears that they are either Laughlin quasiparticles ($K0$) or Skyrmions with very short tails, like the *ad hoc K3*.

Alternatively, the localized state may involve "clumps" of Skyrmions, which result in large Skyrmion-free regions. This may happen, for example, if the disorder potential favors large length scale density fluctuations, subject to the constraint of a collective localization process (see Figs. 2 and 3). More theoretical work is required before this picture can be compared to the data.

For a 2D lattice, the Skyrmion shape consistent with the data is surprising, since the energetics of a *single Skyrmion* state would favor the conventional $K3$ over a shorter tailed Skyrmion (like $K3^*$). However, this preference may not be the same in a *many Skyrmion* state, where the energetics are more complicated. For example, the energy of a single Skyrmion is independent of the phase angle ϕ which defines the global orientation of the XY spin components. In the crystalline phase, however, interactions are generally expected to lead to preferred values for the relative phase angle (ϕ_i-ϕ_j) between the Skyrmions at sites (i, j) [14]. Recent theoretical studies of a square lattice of $K3$ Skyrmions suggested that it was equivalent to the superconducting phase (SC) of the boson Hubbard model [16]. We speculate that the shorter tail of the $K3^*$ Skyrmion would allow ϕ_i, ϕ_j to remain uncorrelated, thereby fixing the number of reversed spins on each site K_i to an integer, which corresponds to the Mott insulating phase (MI) of the boson Hubbard model [19]. If the total energy of this MI phase is lower than the SC phase, the system prefers the $K3^*$ Skyrmion.

[1] T. Chakraborty and P. Pietiläinen, *The Quantum Hall Effects: Integral and Fractional* (Springer-Verlag, Berlin, 1995), 2nd ed.
[2] S. L. Sondhi *et al.,* Phys. Rev. B **47**, 16419 (1993).
[3] For a review, see S. M. Girvin, cond-mat/9907002.
[4] M. Abolfath *et al.,* Phys. Rev. B **56**, 6795 (1997).
[5] H. A. Fertig *et al.,* Phys. Rev. B **50**, 11018 (1994).
[6] S. E. Barrett *et al.,* Phys. Rev. Lett. **74**, 5112 (1995).
[7] E. H. Aifer, B. B. Goldberg, and D. A. Broido, Phys. Rev. Lett. **76**, 680 (1996); M. J. Manfra *et al.,* Phys. Rev. B **54**, 17327 (1996).
[8] Y. Q. Song *et al.,* Phys. Rev. Lett. **82**, 2768 (1999).
[9] A. Schmeller *et al.,* Phys. Rev. Lett. **75**, 4290 (1995).
[10] R. Tycko *et al.,* Science **268**, 1460 (1995).
[11] V. Bayot *et al.,* Phys. Rev. Lett. **76**, 4584 (1996); V. Bayot *et al.,* Phys. Rev. Lett. **79**, 1718 (1997).
[12] D. K. Maude *et al.,* Phys. Rev. Lett. **77**, 4604 (1996).
[13] S. Melinte *et al.,* Phys. Rev. Lett. **82**, 2764 (1999).
[14] L. Brey *et al.,* Phys. Rev. Lett. **75**, 2562 (1995).
[15] A. G. Green, I. I. Kogan, and A. M. Tsvelik, Phys. Rev. B **54**, 16838 (1996).
[16] R. Côté *et al.,* Phys. Rev. Lett. **78**, 4825 (1997).
[17] M. Rao, S. Sengupta, and R. Shankar, Phys. Rev. Lett. **79**, 3998 (1997).
[18] M. Abolfath and M. R. Ejtehadi, Phys. Rev. B **58**, 10665 (1998).
[19] Yu. V. Nazarov and A. V. Khaetskii, Phys. Rev. Lett. **80**, 576 (1998).
[20] C. Timm, S. M. Girvin, and H. A. Fertig, Phys. Rev. B **58**, 10634 (1998).
[21] A. J. Nederveen and Yu. V. Nazarov, Phys. Rev. Lett. **82**, 406 (1999).
[22] S. E. Barrett *et al.,* Phys. Rev. Lett. **72**, 1368 (1994).
[23] P. Khandelwal *et al.,* Phys. Rev. Lett. **81**, 673 (1998).
[24] N. N. Kuzma *et al.,* Science **281**, 686 (1998).
[25] C. P. Slichter, *Principles of Magnetic Resonance* (Springer, New York, 1990), 3rd ed.
[26] A. E. Dementyev, N. N. Kuzma, P. Khandelwal, S. E. Barrett, L. N. Pfeiffer, and K. W. West (to be published).
[27] In this limit, $\mathcal{P}(\nu) = 1 - 2(K + 1)(1 - \frac{1}{\nu})$ for $\nu \geq 1$ and $\mathcal{P}(\nu) = 1 - 2K(\frac{1}{\nu} - 1)$ for $\nu \leq 1$. Experimentally, $K = 2.6 \pm 0.3$ [6].
[28] B. Paredes and J. J. Palacios, Phys. Rev. B **60**, 15570 (1999).
[29] H. Fukuyama and P. A. Lee, Phys. Rev. B **17**, 535 (1978).
[30] J. Sinova *et al.,* Phys. Rev. B **61**, 2749 (2000).
[31] If we assume that $\tau(\mathbf{R_i})$ follows an Arrhenius law, with a spread (ΔU) about the average activation energy (U), we can fit (Fig. 3, solid lines) the $\Gamma_w(T)$ data; $\Delta U/U$ grows from $\sim 1/8$ to ~ 1 as $|\delta\nu|$ increases [26].